Forensic Science International 197 (2010) 70–74

Contents lists available at ScienceDirect

Forensic Science International

journal homepage: www.elsevier.com/locate/forsciint

Forensic differentiation of paper by X-ray diffraction and infrared spectroscopy

Valerio Causin [a,*], Carla Marega [a], Antonio Marigo [a], Rosario Casamassima [b], Giuseppe Peluso [b], Luigi Ripani [b]

[a] Dipartimento di Scienze Chimiche dell'Università, via Marzolo 1, 35131 Padova, Italy
[b] Sezione di Chimica, Esplosivi ed Infiammabili, Reparto Carabinieri Investigazioni Scientifiche, Viale Tor di Quinto 151, 00191 Roma, Italy

ARTICLE INFO

Article history:
Received 10 July 2009
Received in revised form 16 December 2009
Accepted 17 December 2009
Available online 15 January 2010

Keywords:
Forensic science
Questioned documents
Paper
Cellulose
Polymers
IR spectroscopy
X-ray diffraction

ABSTRACT

The possibility to discriminate between sheets of paper can be of considerable importance in questioned document examinations. 19 similar types of office paper were characterized by infrared spectroscopy and X-ray diffraction to individuate the most discriminating features that could be measured by these techniques. The discriminating value associated to them was also assessed. By using a sequence of these two techniques, all the samples could be differentiated.

1. Introduction

The possibility to discriminate between sheets of paper can be of considerable importance in questioned document examinations. In cases in which anonymous letter are involved, for example, the analysis of paper can help to connect or relate different documents, or to compare the threatening letters with the paper seized in the suspect's premises. Document frauds can be carried out substituting a page of an agreement without the consent of all parties. In this instance, the different or common nature of the paper of the questioned page with respect to that of the rest of the document would be a strong point to support or exclude forgery.

A number of techniques have been proposed to carry out such investigations, among which X-ray diffraction [1–4], elemental analysis [5,6], IR spectroscopy [7–9], Raman spectroscopy [10], image analysis [11] and pyrolysis gas chromatography [12]. Physical testing, such as the measurement of density or of mechanical performance, are less viable since they require special apparatus and imply destructive tests. Moreover, they often yield not significant results, given the high standardization of the market and of production procedures, e.g. all common photocopy paper will weigh 80 g/m^2.

Among the testing techniques available in a forensic lab, IR spectroscopy equipped with an Attenuated Total Reflectance (ATR) sampling device is a very attracting method for paper characterization, especially because it allows to perform non-destructive analyses with small sampling depths, i.e. with the possibility of examining the sheet's surface. Kher et al. [8,9] emphasized that IR spectroscopy, coupled with multivariate statistical methods of analysis, is a powerful discriminating tool for the forensic questioned document examiner. They in fact demonstrated that all the samples in a set of six paper varieties could be differentiated by diffuse reflectance (DRIFTS) and 67.86% of the possible pairs within a population of 8 types of paper could be discriminated by ATR [8]. In this article, a very simple quantitative approach to FTIR analysis of paper is presented, which is aimed at the differentiation of a larger population of white sheets of office paper, indistinguishable by visual examination.

XRD is recognized as a valuable technique for studying paper samples [1–4]. Paper is composed of a matrix of cellulose, a natural polymer with linear chains of several hundred to over ten thousand $\beta(1 \rightarrow 4)$ linked D-glucose units. To confer to paper the desired physical–mechanical properties, cellulose is added with a variety of inorganic fillers, the quantity and nature of which are characteristic of each manufacturer. XRD allows to investigate both the polymeric matrix and the inorganic formulation [13,14] of paper composition. On one hand, it is possible to assess the degree of order, i.e. the degree of crystallinity, attained by the cellulose as a consequence of the nature of raw materials and processing

* Corresponding author. Tel.: +39 049 8275153; fax: +39 049 8275161.
E-mail address: valerio.causin@unipd.it (V. Causin).

0379-0738/$ – see front matter © 2009 Elsevier Ireland Ltd. All rights reserved.
doi:10.1016/j.forsciint.2009.12.056

parameters adopted in its manufacturing. On the other hand, it allows also the detection of peaks due to the crystalline structure of inorganic fillers and therefore yields information on the additive profile of the paper sample. Even though forensic document examiners are well aware about the possibilities of this technique to distinguish between paper sheets, recent studies on the discrimination potential of this analytical approach are missing, at least to the knowledge of the authors. One of the aims of this article is to investigate the value and reliability of a differentiation procedure of similar paper samples on the basis of XRD data, and especially its discriminating power. An assessment of this datum is very useful when interpreting results and presenting them to Court.

19 similar types of office paper were characterized by ATR-IR and XRD to individuate the most discriminating features that could be measured by these techniques and to assess the discriminating value associated to them.

2. Experimental

2.1. Samples

A total of 19 reams of white, 80 g/m^2 office paper from different manufacturers were randomly collected from stationery shops in Italy. The samples were designated by a capital letter, the brands of the paper reams used are indicated in Table 1. 5 sheets from different locations within the ream were sampled. A preliminary observation under visible light and ultraviolet examination did not allow to differentiate the samples, i.e. they looked similar in color and texture. The sheets were indistinguishable also by observation under a stereomicroscope, because they showed similarity in the morphology of the constituent fibers.

2.2. Infrared spectroscopy

IR absorption spectra were acquired on a Nexus FTIR spectrometer (Thermo Nicolet) in Attenuated Total Reflection (ATR) mode with a Smart Endurance accessory (Thermo Nicolet) equipped with a diamond ATR crystal and with a ZnSe focusing element. A MIR Globar source was used and the detector was of the DTGS type. The spectral region spanned from 4000 to 650 cm^{-1}, with a resolution of 4 cm^{-1}. The lower limit at 650 cm^{-1} was due to the low detection limit of the employed ATR crystal. In the spectra shown in the rest of this paper, the region between 4000 and 2000 cm^{-1} was not taken into account because in this wavenumber range just the signals due to the O–H groups were present. These are much dependent on the water content of the samples, which is in turn a function also of their storage history. Since this can hardly be controlled, use of these signals in making comparisons was avoided because it could have been misleading.

Both surfaces of each sheet were separately analyzed. Each surface of each of the 5 sheets in every specimen was sampled in at least 5 different locations, and the resulting spectra were averaged by the Nicolet Omnic software bundled to the instrument. Preliminary tests on selected samples showed that increasing the number of sheets and of locations on the same sheet to more than 5 did not significantly increase the precision of the results. It was therefore chosen to apply the above mentioned sampling scheme (5 different locations for 5 different sheets for each ream).

2.3. Wide angle X-ray diffraction

WAXD patterns of the samples were recorded in the diffraction range 10–60° 2θ by a diffractometer GD 2000 (Ital Structures) working in a Seeman-Bohlin geometry and with a quartz crystal monochromator on the primary beam (Cu $K_{\alpha 1}$ radiation). The diffraction patterns were fitted by a least-squares fit procedure elaborated by Hindeleh and Johnson [15]. Samples were mounted in two directions: with the X-ray beam parallel to the width and to the height, respectively, of each paper sheet. In a preliminary phase, three replicates were taken for samples A to E along each direction. It was seen that the repeatability of the measurements was very good and that the obtained diffractograms were superimposable, therefore for subsequent samples just one replicate was done.

3. Results and discussion

3.1. Infrared spectroscopy

Fig. 1 shows an example of the IR spectra that were obtained for paper. These spectra are due to two main components: cellulose, which is the polymeric matrix which constitutes paper, and calcium carbonate, $CaCO_3$, a much used inorganic filler added to confer good physical–mechanical properties. All the considered papers were found to contain $CaCO_3$. No kaolin was detected. This used to be a very common filler used in paper, but it has obviously been displaced in industrial manufacturing by calcium carbonate. Fig. 1 shows the IR spectra due to plain cellulose and pure $CaCO_3$. It can be seen that the most interesting and characteristic absorption features of these two compounds are located in the region between 750 and 1550 cm^{-1}. Calcium carbonate produces a band at about 1420 cm^{-1} and two peaks at 880 and 712 cm^{-1}. These correspond to the asymmetric C–O stretching mode, to the symmetric C–O stretching mode and to the OCO bending (in-plane deformation) modes, respectively, of calcite [16], one of the polymorphs of $CaCO_3$.

Cellulose is characterized in this region by a main band composed by several signals. The peak at 1160 cm^{-1} corresponds to the asymmetric ring breathing, the signal at 1107 cm^{-1} is due to glycosidic C–O–C stretching vibration, and finally the bands at 1055 and 1031 cm^{-1} are due to C–OH stretching vibrations of secondary and primary alcoholic groups of cellulose, respectively [17]. Fig. 1 shows that there is some overlap between the $CaCO_3$ band at 1420 cm^{-1} and some minor peaks of cellulose in the same

Table 1
Characterization data obtained from the IR spectra and the WAXD patterns of the paper samples.

Sample	Brand	R_A	R_B	$C_{\|\|}$	$C_\perp$	Extra peaks (° 2θ)[a]
A	Staples	0.82 ± 0.01	0.82 ± 0.04	58 ± 1	40 ± 1	30.9; 31.4; 41.0
B	Volumax	1.04 ± 0.02	0.67 ± 0.30	49 ± 1	46 ± 1	
C	Viking	0.86 ± 0.05	0.54 ± 0.02	49 ± 1	47 ± 1	31.4
D	Burgo Repro	0.99 ± 0.02	0.70 ± 0.01	48 ± 1	45 ± 1	
E	Xerox	0.95 ± 0.07	0.92 ± 0.01	58 ± 1	50 ± 1	30.9; 31.4
F	Oisco	0.90 ± 0.04	0.84 ± 0.02	48 ± 1	44 ± 1	30.9; 41.0
G	Opportunity	0.95 ± 0.04	0.66 ± 0.01	51 ± 1	36 ± 1	
H	Pigna	0.78 ± 0.02	0.58 ± 0.01	44 ± 1	44 ± 1	
I	Navigator	1.24 ± 0.06	0.53 ± 0.01	58 ± 1	58 ± 1	31.4
J	White Speed	0.68 ± 0.02	0.64 ± 0.04	52 ± 1	47 ± 1	31.4
K	Pigna Ink jet	0.78 ± 0.04	0.68 ± 0.01	52 ± 1	47 ± 1	30.9; 31.4
L	Get Copy	0.86 ± 0.02	0.61 ± 0.04	53 ± 1	44 ± 1	
M	IQ	3.30 ± 1.60	0	55 ± 1	49 ± 1	45.4
N	Regata	0.60 ± 0.06	0.56 ± 0.02	44 ± 1	29 ± 1	31.4
O	Fabriano	1.16 ± 0.04	0.55 ± 0.03	54 ± 1	52 ± 1	31.4
P	Copy Blu	0.66 ± 0.02	0.59 ± 0.03	48 ± 1	32 ± 1	31.4
Q	Golden Plus	0.67 ± 0.04	0.65 ± 0.01	53 ± 1	42 ± 1	
R	Diatec Group	0.20 ± 0.01	0.14 ± 0.01	44 ± 1	31 ± 1	See Fig. 6: starkly different inorganic profile
S	Golden Star	0.41 ± 0.03	0.38 ± 0.03	51 ± 1	50 ± 1	31.4

[a] In this column just the peaks in addition to those of $CaCO_3$ (which were present in all the samples) are shown.

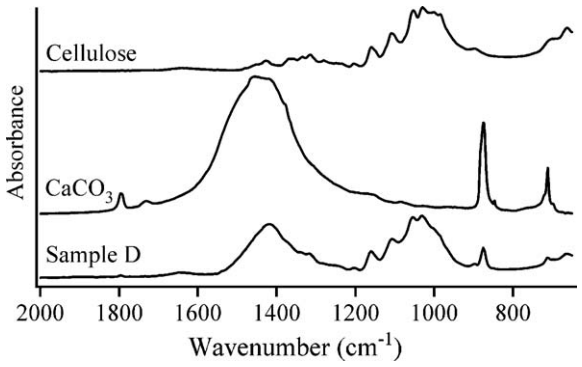

Fig. 1. IR spectra of sample D, and of reference cellulose and $CaCO_3$.

region. It was nevertheless decided to take the asymmetric C–O stretching vibration of $CaCO_3$ into account for the quantitative procedure of IR data treating. Its molar absorptivity was in fact much higher than that of the signals of cellulose in the same spectral range, and therefore it could be assumed that the intensity of that peak in the paper spectrum was principally ascribable to $CaCO_3$ content. As a measure of cellulose content, the intensity of the bands between 915 and 1200 cm^{-1} was integrated, obtaining the area, denominated in the following of this paper as A^{Cell}. The amount of $CaCO_3$ was quantified by measuring by integration the area $A_{880}^{CaCO_3}$ of the peak at 880 cm^{-1} (symmetric C–O stretching mode) and the area $A_{1420}^{CaCO_3}$ of the peak at 1420 cm^{-1} (asymmetric C–O stretching mode). The $CaCO_3$ peak at 712 cm^{-1} was not considered because it overlapped the rising baseline of cellulose towards small wavenumbers.

The peaks were preliminarily integrated with two methods [18,19]. In the first, the integration limits were selected at the minima on each side of the absorption band. This technique was not satisfactory, because when the baseline was sloping or noisy, no minima could be present and the limits had to be evaluated subjectively. The second method, the one used to determine the results presented in this paper, made use of the same integration limits for all the samples. The two $CaCO_3$ peaks were integrated in the ranges 1550–1250 and 915–820 cm^{-1}. Integration of the cellulose peak was performed between 1200 and 915 cm^{-1}. A ratio was then computed dividing the sum of the peak areas due to $CaCO_3$ by the area of the cellulose, i.e.:

$$R = \frac{A_{880}^{CaCO_3} + A_{1420}^{CaCO_3}}{A^{Cell}}$$

R was calculated for both sides of the considered sheet. The side with the largest R was conventionally denominated side A.

Table 1 shows the obtained data, which are visually represented in Fig. 2. Some of the specimens did not show appreciable differences between the two sides of the sheet, whereas in some cases the two sides differed considerably for the relative content of $CaCO_3$ and cellulose. This may be ascribed to different manufacturing procedures that determine an uneven distribution of the filler in the cellulose matrix. The different errors that affect R_A and R_B for the same sheet should also be ascribed to the production process. In other words the sheet of paper does not experience exactly the same processing conditions on both sides, and this is reflected by more or less pronounced differences in the composition of the two surfaces. A good differentiation of the samples based on R_A and R_B values was possible. To quantify the discriminating power (DP) of the technique, the approach of Smalldon and Moffat was applied, i.e. the ratio between the number of differentiated pairs over the number of possible pairs was calculated [20]:

$$\mathrm{DP} = \frac{\text{number of differentiated sample pairs}}{\text{number of possible sample pairs}}$$

The number of possible sample pairs was $[n\cdot(n-1)]/2$, where n is the total number of samples, i.e. $n = (19 \times 18)/2 = 171$.

Four sample pairs, i.e. J and Q, J and P, N and P and I and O had indistinguishable R_A and R_B values, within the experimental error. Therefore, 97.6% of possible sample pairs could be successfully discriminated by at least one of the two ratios, R_A and R_B.

XRD was applied in a twofold manner. On one hand, focus was posed on the cellulose matrix, on the other hand, the inorganic filler profile was investigated. Cellulose is found in a number of different varieties, generally named cellulose I, II, III and IV. Of these, cellulose I is the one commonly encountered in nature [3]. The currently accepted model for the crystalline structure of cellulose I proposes the existence of two crystal forms, triclinic I_α and monoclinic I_β [21]. The proportion of the two polymorphs varies in the different plants: higher plants like cotton have predominantly I_β phase, on the contrary, the lower forms of cellulose are dominated by the metastable I_α form [21]. In the textile industry, a transition from cellulose I to cellulose II is obtained by the mercerization process, in which cotton is treated with strong alkali to correct some undesirable properties of cellulose I such as bad elasticity or low dyeability, due to the high crystallinity and orientation of cellulose I [22]. The X-ray diffraction spectrum of paper is very broad and diffused, and consists of a main peak located at about 22.7° 2θ with a shoulder at around 22° 2θ and of three secondary maxima at 14.8°, 16.3° and 20.3° 2θ (Fig. 3). The characteristic peaks of cellulose I are located at 14.8°, 16.2° and 22.7° 2θ [3,22,23]. Cellulose II yields XRD peaks at 20.2° and 21.8° 2θ [22,23]. The characteristic reflections of cellulose I_α and I_β are overlapped [24,25]. Fig. 3

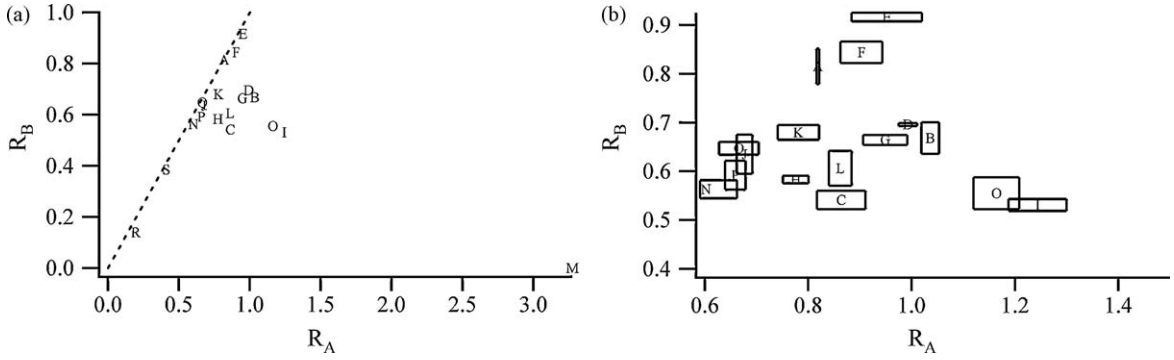

Fig. 2. Plot of R_B vs. R_A for (a) all the considered samples, and (b) with a magnified scale on the cluster where most of the samples are concentrated. The dotted line is a line of unit slope, intended to show the behavior of sheets with the same R on both sides. Boxes are used to represent error bars.

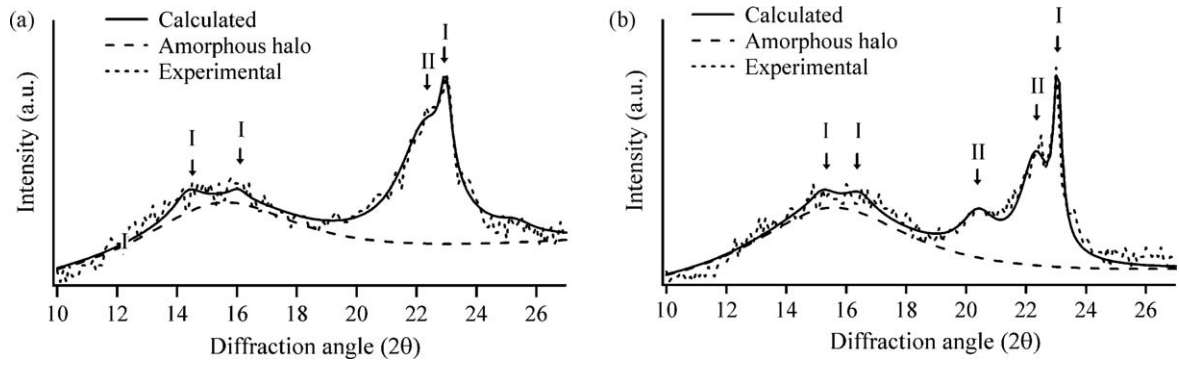

Fig. 3. WAXD spectra of samples (a) A and (b) P in the angular range relative to cellulose. All the samples were mounted in the perpendicular direction. The indexes of the major reflections of cellulose I and II are indicated. Calculated patterns are also shown.

shows a coexistence of both cellulose I and II. Strong alkali such as NaOH are in fact used in the manufacturing process of pulp and paper, and it is known that a cellulose I → cellulose II transition is induced at high pH values [22,23]. Moreover, Foner and Adan [3] showed that mechanical treatments, normally employed in the pulp and paper industry, such as grinding or beating, bring about severe modifications of the WAXD profile, i.e. cellulose peaks are much smoothed and broadened. The qualitative appearance of the WAXD spectra of different papers, an example of which is shown in Fig. 3, therefore reflects the process parameters that were applied in their production. The quantification of such effects was made by assessing the degree of crystallinity of the polymer. Cellulose, as many polymers, is semicrystalline in nature. Due to entropic constrains, in fact, its large macromolecular chains are unable to form a crystalline lattice extended to the whole sample, as it happens with low molecular weight molecules. The structure and morphology of cellulose is therefore better described as an alternation of crystalline and amorphous domains. Each of these regions contributes to the WAXD pattern: crystalline domains originate rather sharp Bragg reflections, whereas the amorphous zones produce a wide and diffused halo. A fitting procedure of the experimental patterns was performed, by which the contributions of the crystalline and amorphous domains was deconvoluted (Fig. 3). An amorphous halo of fixed width and position was used in order to assure the comparability of results. Crystallinity was thus evaluated as the ratio between the area of crystalline peaks over the total area of the diffractograms. The angular range in these calculations was limited between 10° and 27° 2θ because, at wider angles, signals due to fillers and additives appeared, that could interfere with the polymer peaks. As described in Section 2, acquisitions were performed along two different directions. The one yielding the most crystalline pattern will be denoted in the rest of this paper as the parallel pattern and designated with the symbol ||, the other one will be indicated as perpendicular, ⊥. The reason for adopting a convention like this is that the single sheets can be cut from a larger sheet along the machine or transversal direction, and sheets of both these types can be present in the same ream. Fig. 4 shows that the orientation induced by the manufacturing process can be detected on the basis of the different WAXD patterns from the same sample mounted in these two directions. These qualitative differences are translated in the quantitative differences between the degrees of crystallinity along the parallel, $C_{||}$, and perpendicular, $C_{\perp}$, directions (Table 1 and Fig. 5). Eight sample pairs, i.e. B and C, B and D, B and F, C and D, D and F, J and K, L and Q and N and R had indistinguishable $C_{||}$ and $C_{\perp}$, within the experimental error. Therefore, 95.3% of possible sample pairs could be successfully discriminated by at least one of the two crystallinity degrees.

Another feature that characterized the WAXD patterns of the considered samples was the appearance of sharp peaks not attributable to the polymer, but ascribable to crystalline fillers added to modulate the mechanical properties of paper (Fig. 6). All the samples showed all the characteristic peaks of $CaCO_3$ in the calcite form, i.e. the peaks at 29.4°, 36.0°, 39.4°, 43.2°, 47.5°, 48.5°, 56.6° and 57.4° 2θ [26]. Minor peaks, probably due to additives present in very small amounts, appeared for some samples, and proved very useful for their differentiation. Sample R was particularly different from the other specimens, because it showed a starkly different inorganic profile. In addition to the calcite peaks, in fact, a number of other very intense reflections appeared in its diffractograms, making it a very peculiar sample in the considered population. It is interesting to note that in no sample the characteristic peak of kaolin at 12.4° 2θ appeared, signifying that

Fig. 4. WAXD spectra of sample N mounted in the parallel (top) and perpendicular (bottom) directions, in the angular range relative to cellulose.

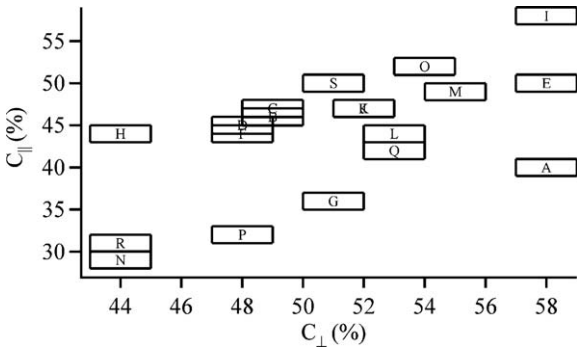

Fig. 5. Plot of $C_{||}$ vs. $C_{\perp}$ for all the considered samples. Boxes are used to represent error bars.

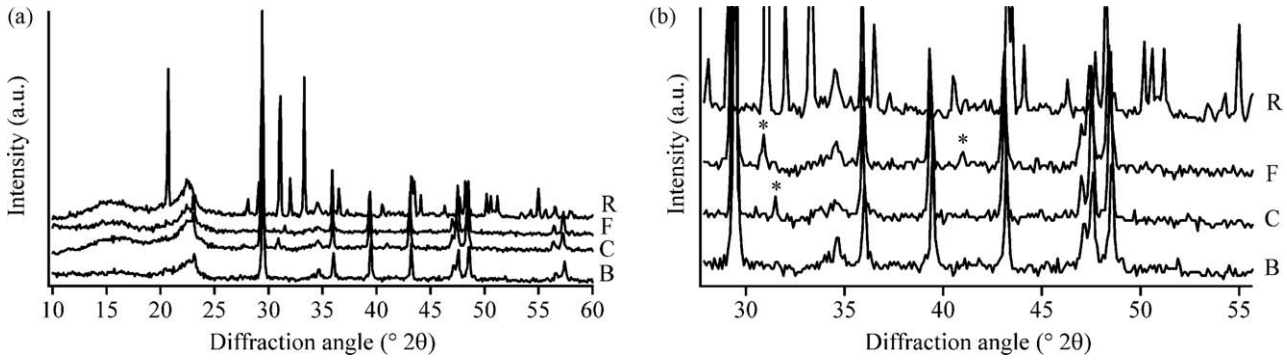

Fig. 6. WAXD spectra of samples B, C, F and R (a) in the whole angular range and (b) magnifying the region of the inorganic peaks. Minor peaks useful for differentiation of the samples are indicated by *. All the samples were mounted in the perpendicular direction.

this additive is no longer used at least in the Italian, and probably European market.

It is worth considering that the profile due to the inorganic content of paper was the same, in terms of position and of relative intensities of the peaks, regardless of the direction in which the sample was mounted. This means that the composition of the fillers was very homogeneously distributed along the plane of the paper. So the production process can produce an uneven distribution of inorganic additives along the thickness of the sheet, as evidenced by FTIR, but not in the plane of the paper.

The profile due to inorganic peaks (Table 1) allowed to differentiate all the couples but one, B and D, that had resulted indistinguishable by the degree of crystallinity. The overall DP associated to the XRD analysis of these paper samples was therefore 0.99. More importantly, the simultaneous application of both these techniques allowed to differentiate all the samples.

Although the present work was focused on the discrimination potential of XRD and IR applied on paper, some blind tests were also performed to check the value of the method in identification. Three samples were taken from the sheets that had already been analyzed in the previous part of the work. These blind samples were analyzed, by an operator that had not participated in the previous part of the work, 8 months after the completion of the measurements aimed at studying the discrimination potential. Blind samples were correctly identified, because there was agreement, within the experimental error, of R_A, R_B, $C_{||}$, $C_{\perp}$, and the peaks due to inorganic additives. Although a systematic study in this direction was not carried out, indications that this procedure can provide useful data also for identification purposes were obtained.

4. Conclusion

A discrimination procedure for paper samples based on IR spectroscopy and XRD was presented. All the samples out of a population of 19 papers, indistinguishable by visual examination, could be discriminated. This result was achieved by a non-destructive technique, requiring very easy and immediate data treatment. These two techniques allowed to detect the variations in the structure brought about by different processing parameters, manufacturing conditions and formulation of additives.

References

[1] D. Ellen, The Scientific Examination of Questioned Documents. Methods and Techniques, Taylor and Francis, London, 1997.
[2] J.S. Kelly, B.S. Lindblom, Scientific Examination of Questioned Documents, 2nd ed., Taylor and Francis, Boca Raton, FL, 2006.
[3] H.A. Foner, N. Adan, The characterization of papers by X-ray diffraction (XRD): measurement of cellulose crystallinity and determination of mineral composition, J. Forensic Sci. Soc. 23 (1983) 313–321.
[4] J. Levinson, Questioned Documents: A Lawyer's Handbook, Academic Press, London, 2001.
[5] L.D. Spence, A.T. Baker, J.P. Byrne, Characterization of document paper using elemental compositions determined by inductively coupled plasma mass spectrometry, J. Anal. Atom. Spectrom. 15 (2000) 813–819.
[6] L.D. Spence, R.B. Francis, U. Tinggi, Comparison of elemental composition of office document paper: evidence in a homicide case, J. Forensic Sci. 47 (2002) 648–651.
[7] J. Andrasko, Microreflectance FTIR technique applied to materials encountered in forensic examination of documents, J. Forensic Sci. 41 (1996) 812–823.
[8] A. Kher, M. Mulholland, B. Reedy, P. Maynard, Classification of document papers by infrared spectroscopy and multivariate statistical techniques, Appl. Spectrosc. 55 (2001) 1192–1198.
[9] A. Kher, S. Stewart, M. Mulholland, Forensic classification of paper with infrared spectroscopy and principal component analysis, J. Near Infrared Spectrosc. 13 (2005) 225–229.
[10] A.H. Kuptsov, Applications of Raman spectroscopy in forensic science, J. Forensic Sci. 39 (1994) 305–318.
[11] H. Miyata, M. Shinozaki, T. Nakayama, T. Enomae, A discrimination method for paper by Fourier transform and cross correlation, J. Forensic Sci. 47 (2002) 1125–1132.
[12] H. Ebara, A. Kondo, S. Nishida, Analysis of coated and non-coated papers by pyrolysis gas-chromatography, Rep. Natl. Res. Inst. Police Sci. 2 (1982) 88–98.
[13] V. Causin, C. Marega, P. Carresi, S. Schiavone, A. Marigo, A quantitative differentiation method for plastic bags by wide angle X-ray diffraction for tracing the source of illegal drugs, Forensic Sci. Int. 168 (2007) 37–41.
[14] V. Causin, C. Marega, A. Marigo, When polymers fail: a case report on a defective epoxy resin flooring, Eng. Failure Anal. 14 (2007) 1394–1400.
[15] A.M. Hindeleh, D.J. Johnson, The resolution of multipeak data in fiber science, J. Phys. D: Appl. Phys. 4 (1971) 259–263.
[16] F.A. Andersen, L. Brečević, Infrared spectra of amorphous and crystalline calcium carbonate, Acta Chem. Scand. 45 (1991) 1018–1024.
[17] J. George, V.A. Sajeevkumar, R. Kumar, K.V. Ramana, S.N. Sabapathy, A.S. Bawa, Enhancement of thermal stability associated with the chemical treatment of bacterial (Gluconacetobacter xylinus) cellulose, J. Appl. Polym. Sci. 108 (2008) 1845–1851.
[18] M.W. Tungol, E.G. Bartick, A. Montaser, Forensic analysis of acrylic copolymer fibers by infrared microscopy, Appl. Spectrosc. 47 (1993) 1655–1658.
[19] V. Causin, C. Marega, G. Guzzini, A. Marigo, Forensic analysis of poly(ethylene terephthalate) fibers by infrared spectroscopy, Appl. Spectrosc. 58 (2004) 1272–1276.
[20] K.W. Smalldon, A.C. Moffat, The calculation of discrimination power for a series of correlated attributes, J. Forensic Sci. Soc. 13 (1973) 291–295.
[21] R. Chen, K.A. Jakes, D.W. Foreman, Peak-fitting analysis of cotton fiber powder X-ray diffraction spectra, J. Appl. Polym. Sci. 93 (2004) 2019–2024.
[22] Y. Liu, H. Hu, X-ray diffraction study of bamboo fibers treated with NaOH, Fibers Polym. 9 (2008) 735–739.
[23] M.A. Moharram, O.M. Mahmoud, X-ray diffraction methods in the study of the effect of microwave heating on the transformation of cellulose I into cellulose II during mercerization, J. Appl. Polym. Sci. 105 (2007) 2978–2983.
[24] M. Wada, T. Okano, Localization of Iα and Iβ phases in algal cellulose revealed by acid treatments, Cellulose 8 (2001) 183–188.
[25] Z. Yan, S. Chen, H. Wang, B. Wang, J. Jiang, Biosynthesis of bacterial cellulose/multi-walled carbon nanotubes in agitated culture, Carbohydr. Res. 74 (2008) 659–665.
[26] H. Effenberger, K. Mereiter, J. Zemann, Crystal structure refinements of magnesite, calcite, rhodochrosite, siderite, smithsonite, and dolomite, with discussion of some aspects of the stereochemistry of calcite type carbonates, Z. Kristallogr. 156 (1981) 233–243.